Fusion of Multiple View Interferometric and Slant Range SAR Data for Building Reconstruction

Regine Bolter[a] and Franz Leberl[a]

[a]Computer Graphics and Vision, Graz University of Technology
Inffeldgasse 16/2, A-8010 Graz, Austria

ABSTRACT

Modern very high resolution interferometric SAR sensors deliver slant range magnitude and ground range interferometric height and coherence measurements at pixel sizes of 30cm to 10cm from a single flight path. Detection and reconstruction of buildings get feasible from this kind of data. Single data sources are corrupted by blur, speckle noise and other view dependent effects as e.g., layover and shadows. Especially in case of buildings, those phenomenological features provide also valuable information about the underlying building structure. In this paper we use information from the interferometric height and coherency channel to detect buildings. Shadow information from slant range magnitude images is then used to delimit the exact boundaries of the buildings further and rectangles are fit to the selected points. The resulting building models are input into a simulator to produce slant range magnitude images and interferometric height information. The layover and shadow regions from this simulated images are compared with the corresponding regions in the original data to detect occlusions of adjacent buildings and to further refine the building structure. The results are compared to ground truth data available from optical imagery. Accuracies achieved in the measurement of building dimensions are in the range of 3 pixels.

Keywords: multiple view fusion, multiple datatype fusion, IFSAR, building reconstruction

1. INTRODUCTION

The advent of very high resolution radar images at pixel sizes of 30cm and smaller has intensified the interest in using radar images for topographic mapping at reasonably large scale, specifically addressing human scale objects, as e.g., roads, buildings or fences, which were not available reliably from radar images until now. Additionally radar interferometry promises a significant improvement in the automated analysis of radar images, and in obtaining three-dimensional data about the world. Due to the all-weather/day- night applicability of SAR sensors multiple views over a short time can be easily obtained. Multiple views add the opportunity to use additional shape-from-X methods to enhance robustness, accuracy and completeness, but require an ability to overcome geometric disparities and radiometric dissimilarities.

Detection and reconstruction of buildings from remote sensing data requires high resolutions, which were not available until recent from SAR sensors. Therefore the literature on this topic is limited. However, some interesting approaches were presented, most of them based on the exploitation of interferometric information, rather than on the basic magnitude images. Ref. 1 describes an automatic region growing approach applied to interferometric height data to localize buildings starting from the shadows they cast. In Ref. 2 fusion of IFSAR and multispectral optical image data results in bounding boxes of buildings. Geometrical considerations on the interferometric imaging process in Ref. 3 lead to an approach to enhance the quality of IFSAR height measurements of buildings. Several segmentation algorithms applied to interferometric height data can be found. For example, Ref. 4 reconstruct the slopes of urban tower blocks from IFSAR height data by first applying a range segmentation algorithm[5] developed for general range images. Another segmentation algorithm for building detection applied to interferometric height data is described by Ref. 6. Most of the work discussed until now concentrates on the exploitation of interferometric height information. The combination of information from segmented magnitude SAR images with interferometric height data to enhance the height data of buildings is shown in Ref. 7, and the proper visualization of the achieved results are presented in Ref. 8.

All these previous demonstrations were performed on single type data. We want to employ the best source available for each single measurement and combine the results in an intelligent way.

Further author information: (Send correspondence to R.B.)
R.B.: E-mail: bolter@icg.tu-graz.ac.at
F.L.: E-mail: leberl@icg.tu-graz.ac.at

2. CONCEPT

The overall concept of our building detection and reconstruction strategy from multiple view/multiple data type interferometric SAR data is depicted in Fig. 1. To study the various and mostly view dependent effects present in IFSAR measurements of buildings and their dependence on the geometric parameters in detail, a single pass IFSAR simulator is a valuable tool. From simulated data the information contained in each single type data will be segmented and grouped in order to reconstruct the actual scene geometry from single data type, multiple view simulated data. In a further step, the results from single data type measurements have to be fused. The same procedures are then applied to the original SAR data. Each single data type is exploited using the methods developed for simulated data and finally the results from all single data types are fused. Feeding the resulting building models back into the simulator and comparing the resulting simulation to the original data could establish a feedback loop to further enhance the model. Especially view dependent effects such as layover areas or occluded shadow regions can be identified and excluded from the original data for further processing.

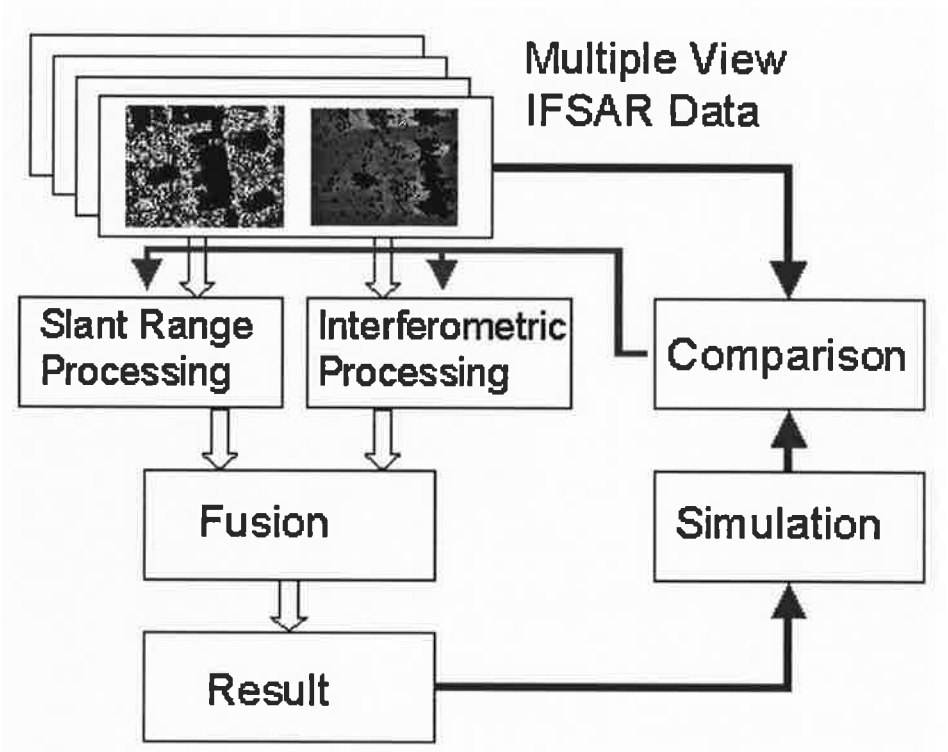

Figure 1. Overall building detection and reconstruction concept.

3. TEST DATA

For the detection and reconstruction of buildings test data from the McKenna MOUT site, Ft.Benning, GA is used. The buildings on this site are clustered in a compact group resembling a northern European village, surrounded by undeveloped land. An optical image of the testsite can be seen from Fig. 2. From an airborne Sandia Spotlight IFSAR sensor the testsite was imaged from four cardinal azimuth directions. The original slant range magnitude images have a resolution of 0.3 m. A subsection of an original slant range SAR magnitude image can be seen from the left of Fig. 6. The interferometric processing was done by Sandia, each pass was processed into four channels: magnitude, correlation, height and bin number, and converted to UTM coordinates with a resolution of 0.4 m.

An ARC/INFO data set of the Fort Benning MOUT site is used as the ground truth to evaluate the building extraction results. This data set contains the UTM coordinates of building corners, building areas, perimeter as well as building heights, etc.

Figure 2. Optical Image of the Ft. Benning MOUT testsite.

4. METHODS

To study the various effects present in SAR data we set up a work environment with a simulator to produce slant range and interferometric SAR data. The slant range magnitude simulator and the reconstruction of a single house from shadows casted in multiple view simulated and real data is presented in Ref. 9. The extension of our simulator to produce single pass interferometric phase and height information is described in more detail in Ref. 10.

4.1. Building Detection from Interferometric Height Information

Interferometrically derived digital elevation models suffer from effects of image blur, speckle, layover and shadow. These effects are depending on illumination direction; therefore a combination of information gained from multiple directions, for example the four cardinal azimuth directions, is useful to enhance the IFSAR DEM.

For the interferometric height data, shadow results in an area of no values facing away from the backslope of an object, and layover results in the so called "front porch" anomaly.[3] This effect results from the superposition of multiple scatterers in layover areas and appears as an extended region on the near-range side of an object that is characterized by altitudes in between the values on the ground and the values on the objects top. The front porch enlarges the building towards the sensor, the height values around the front wall inside the building are lower than expected.

For the combination of multiple views of interferometric height information, a simple maximum decision strategy seems feasible: For each pixel in the scene, the maximum height value over all independent measurements is chosen. Figure 3 shows this multiple view maximum combination for a subscene of interferometric height data. Due to the front porch effect this may result in larger building areas than actually the case, and quite noisy object borders. However, this strategy makes the detection of even small buildings possible.

Applying a large area minimum filter to this multiple view combined height map, a decision between bare earth and objects rising up from this bare earth could be drawn. Subtracting the resulting bare earth from the height map and applying a single threshold delivered a binary mask, where all objects rising up from the bare earth by more than the threshold were selected. From this binary mask startpoints for regions of interest, where buildings are supposed to be, were selected using morphological operations, minimum bounding rectangles around this start regions were calculated. More details about this procedure can be found in Ref. 11.

The differentiation between buildings and other objects rising up from the bare earth, e.g., trees, bushes, can not be drawn from the height measurements alone. Therefore during the height map combination step a corresponding combined coherency map was computed. For each position in the map, the coherency value corresponding to the

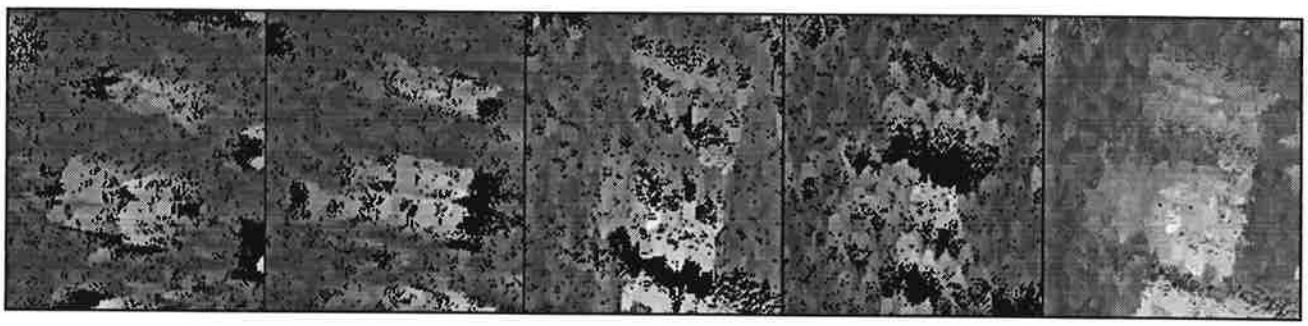

Figure 3. From left to right: interferometric height data for two buildings from four independent views and "maximum" combination of these four views on the right. The area covers approximately 50 x 60 m^2.

selected maximum height value was chosen. Simple texture measures in the selected region from the height and coherency information were evaluated, therefrom a decision between natural and man-made objects rising up from the bare earth was drawn.

4.2. Building Reconstruction from Slant Range SAR Images

Another approach to infer height measurements from radar data is based on shadows cast in the slant range images. From position and length of shadows in a single slant range SAR image, one can calculate the position and height of all walls facing away from the sensor. The principle is described in Ref. 9. The accurate segmentation of the shadow boundaries is the crucial task for an exact reconstruction.[12] This was accomplished using a rotating mask with a simple transition between two regions for edge detection. For each of the 16 rotation steps, mean and variance of the intensity within the two regions were calculated separately and the differences were exploited. From the segmented shadow areas position and height of the back wall of the object which caused the shadow could be calculated. Measurements resulting from independent views can be combined. This results in point clouds which resemble the

Figure 4. Reconstructed building walls of the whole building ensemble on the MOUT testsite with overlaid building outlines from ground truth data. The area covers approximately 180 x 150 m^2.

buildings outlines, as can be seen from Fig. 4. These buildings outlines are quite fuzzy defined, various gaps and outliers exist due to noise still present in the segmented shadow areas and especially due to occlusions, when adjacent buildings interfere with the shadow regions of the actual building as can be seen for the buildings F and G. Another problem occurs at the endpoints of each wall, where layover effects superimpose the shadow areas, this effect is especially visible for the buildings A, C and L in Figure 4.

Using the information about where buildings are supposed to be obtained from interferometric data, the point clouds were grouped into 15 distinct buildings and rectangles were fit to these point clouds. For each point in the point cloud the distance to the nearest point on the rectangle was calculated for all reasonable rectangles and the rectangle with the minimum overall quadratic distance error was chosen.

4.3. Combination of Multiple Data Type Results

The buildings outlines can be measured more accurately from slant range shadows than from interferometric height data. On the other hand, the buildings height inside the buildings footprints is better defined from interferometric height data. The fusion of these two data sources enhances the resulting building models. Simple rectangle blocks are used to model the buildings. The rectangles fit to the footprints resulting from slant range SAR shadows were used as starting point for the building models, the mean height value from the combined interferometric height map was calculated within these rectangles and assigned to the building model. Fig. 5 shows a shaded view of the resultant first model for the whole testsite.

4.4. Comparing the Model to Real Data Using Simulation

This first model with rectangular buildings was input to our single pass interferometric SAR image simulator[9,10] The parameters for the simulation where chosen to match the parameters used by the real sensor, four cardinal azimuth views over the testsite were computed. The resulting slant range magnitude SAR images and interferometric height measurements were compared to the original data.

A comparison between original and simulated slant range magnitude images for a single view can be seen from Fig. 6. The simulation uses a rather simple radiometric model, the visible differences between real and simulated images are evident, especially because no thematic content, as e.g., road and pavement properties, roof materials, etc., was considered for the simulation. Another striking difference between the two images is the missing speckle

Figure 5. First site model with simple rectangular building blocks resulting from the combination of information from slant range shadows and interferometric height measurements. The area covers approximately 220 x 220 m^2.

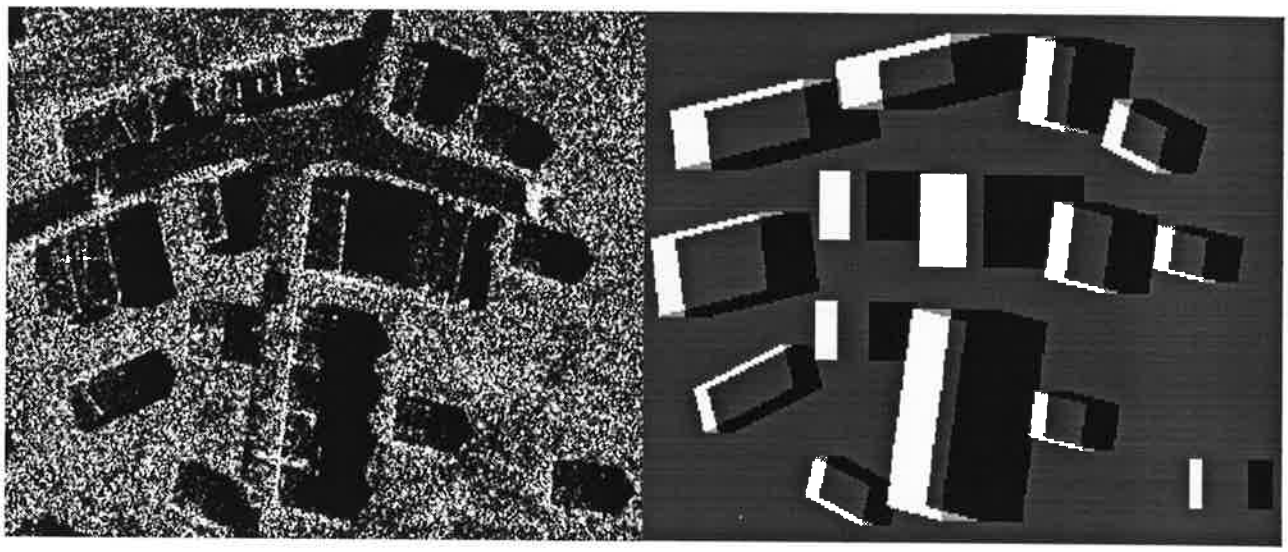

Figure 6. Subsection of original slant range magnitude image over the MOUT testsite on the left and the corresponding simulation using the extracted model from Fig. 5 on the right. The area covers ca. 150 x 90 m^2.

noise in the simulated image. Adding speckle noise with the appropriate statistical model to get a more close visual fit would be no problem. However, we are interested especially in the manifestations of layover and shadow phenomena in the simulated images in comparison to the real data, speckle effects would complicate the identification of such regions.

4.5. Shadow Occlusion Detection

Comparing the black shadow regions between real and simulated data in Figure 6 the differences between the simple rectangular building models used for the simulation and the actual buildings become visible. One possibility would be to exploit this shape differences to enhance the building model. On the other hand the layover regions are quite

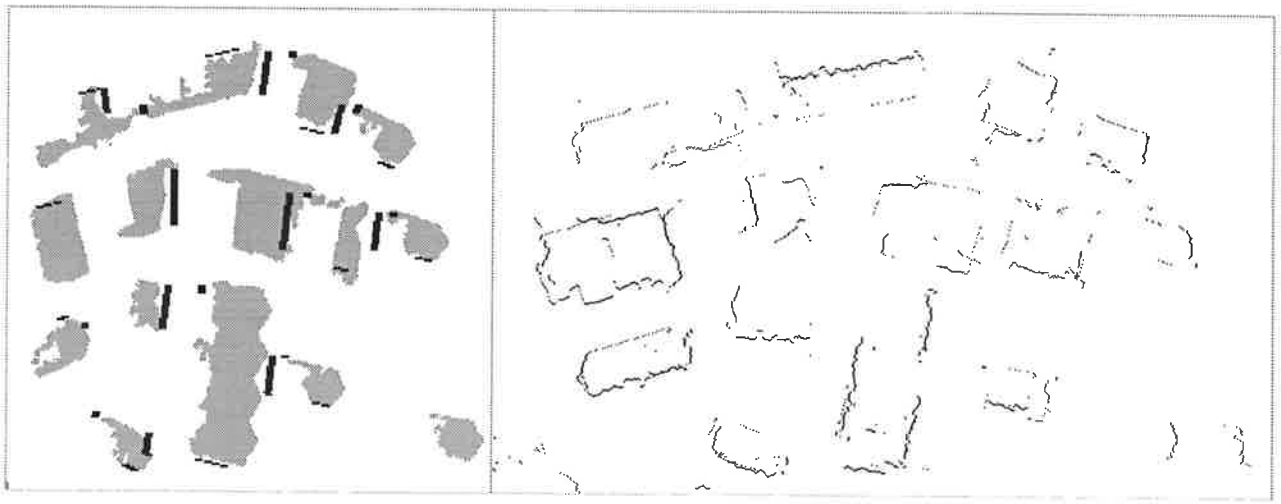

Figure 7. On the left: Segmented shadow areas from the original slant range image shown on the right of Fig. 6 with occlusions marked according to the layover/shadow boundaries in the simulated data. On the right: Resulting footprints of building walls after the shadow correction procedure. The area covers approximately 150 x 90 m^2.

evident from the simulated data and it can be seen that the shadow region is disturbed wherever layover regions border shadow regions. Two different cases occur, if a building is not oriented perpendicular to the flight direction at the outer corners layover regions are succeeded by shadow areas as seen from the sensor, where the cross section of the building in range direction is thinner than the layover depth caused by the building's front wall. The second case are real occlusion, when adjacent buildings interfere with the shadow casted from the actual building. In this case shadow regions are succeeded by layover areas.

Fig. 7 shows on the left the segmented shadow areas from the original slant range image shown on the right of Fig. 6 where the occlusions are marked according to the layover/shadow boundaries in the simulated data. The black stripes mark shadow occlusions due to the orientation of the building, dark grey stripes mark the areas where real occlusion occur. Using this knowledge it is possible to exclude this occluded shadow lines from further exploitation to enhance the analysis. The resulting footprints of the reconstructed walls after this correction procedure can be seen from Fig. 7 on the right.

4.6. Front Porch Removal

The correct simulation of interferometric height measurements in layover areas requires some extra calculation.[10] During this simulation process it is possible to compute a layover map corresponding to the ground range geometry of the resulting height values. Because our simulator is geometrically accurate, the layover maps can be superimposed directly to the original ground range height maps. In section 4.1 the combination of multiple views of interferometric height data to form a single map was described. A simple maximum decision strategy was used to combine the values. For each pixel in the resulting height map the maximum over all height values of the individual views at the same location was chosen. The result of this maximum height combination can be seen from Fig. 8 on the right. This procedure enabled the detection of even small buildings, however, due to the front porch effect the buildings areas were enlarged through this procedure and the buildings outlines got quite fuzzy.

From the simulation of interferometric height information from the first model extracted from our data we now know where these front porch areas, caused by layover phenomena, are supposed to be. Therefore now a different combination strategy can be applied: The corresponding layover map is superimposed to each single view of the original interferometric height measurements, and pixels in this single views are only valid, if no layover or shadow occurs on this position. In contrast to the slant range magnitude images, the shadow pixels in the interferometric height measurements are indicated by a special negative value. For each pixel the mean value over all valid height values at the same position in the individual views is calculated and assigned to the resulting combined height map.

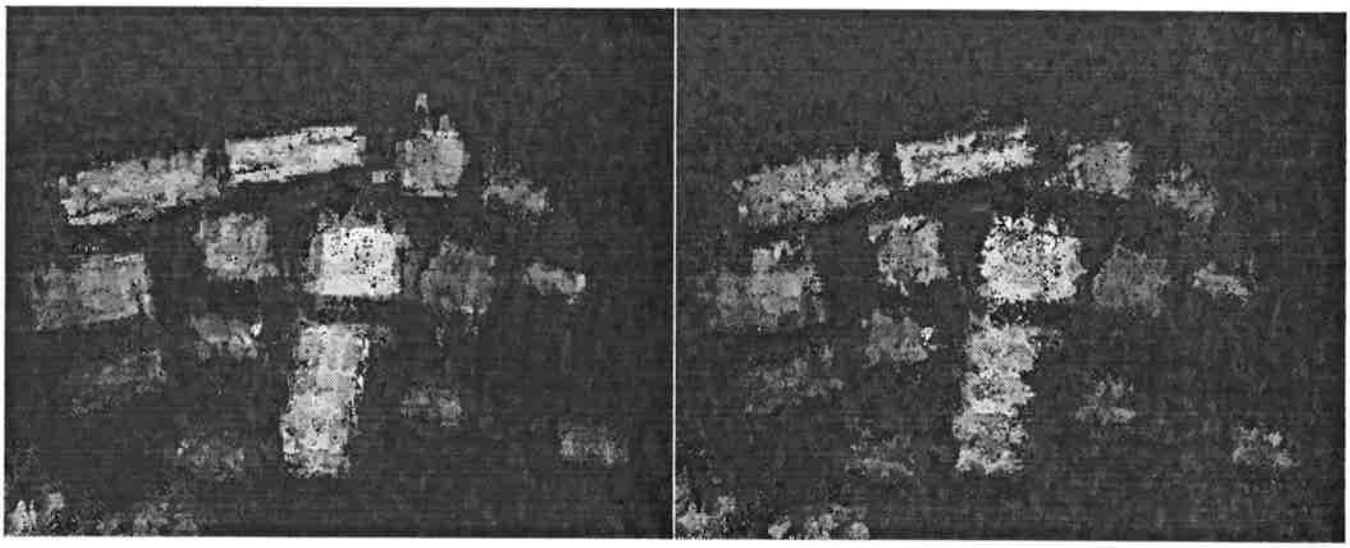

Figure 8. Resulting combined height map after front porch removal on the left and for comparison the maximum combined height map without front porch removal on the right.The area covers approximately 160 x 120 m^2.

There are positions, where no valid height values occur, in this case the maximum height value over all independent views is chosen to avoid gaps in the resulting height map. The result of this front porch removal procedure can be seen from Fig. 8 on the left. On the right once more the simple maximum fusion applied in Sect. 4.1 is shown for comparison. The appearance of the front porch removed height map is more smooth than the maximum combined height map due to the averaging over valid height values, building's edges appeear sharper.

5. RESULTS

Using the rectangles fit to the reconstructed walls from shadow as buildings outlines and the height values from the front porch corrected combined interferometric map we are now able to fit simple building models to this segmented points. The two most basic building models are flat roofed and symmetric gable roofed. Using all height values inside the optimal rectangle calculated from the shadow boundaries we calculated the mean height value for the flat roof type building. Then the rectangle was split up in the middle and planes were fit parallel to the axis to each half. This was done for both directions of the rectangle. The planes fit to each half were mirrored to the other half to get symmetric gable roofs. The result of this procedure are 5 building models, a flat roof parallel to the ground plane and four different symmetric gable roofed models. For each of the 5 models the RMS error between the original height values and the planes of the model is calculated and the model with the minimum RMS error is chosen. The resulting building model for our testsite can be seen from Fig. 9. Figure 10 shows for comparison the ground truth data of the same testsite in a similar view.

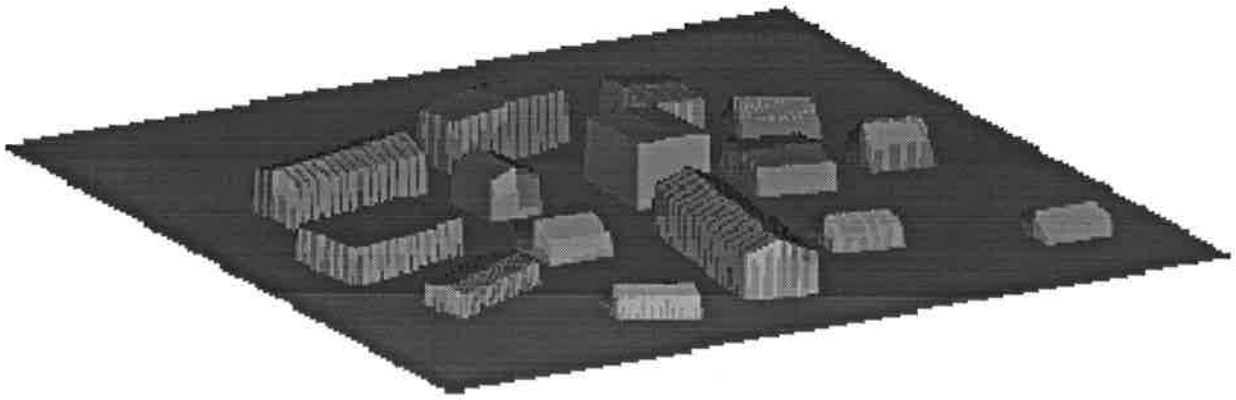

Figure 9. Shaded view of the resulting site model. The area covers approximately 160 x 120 m^2.

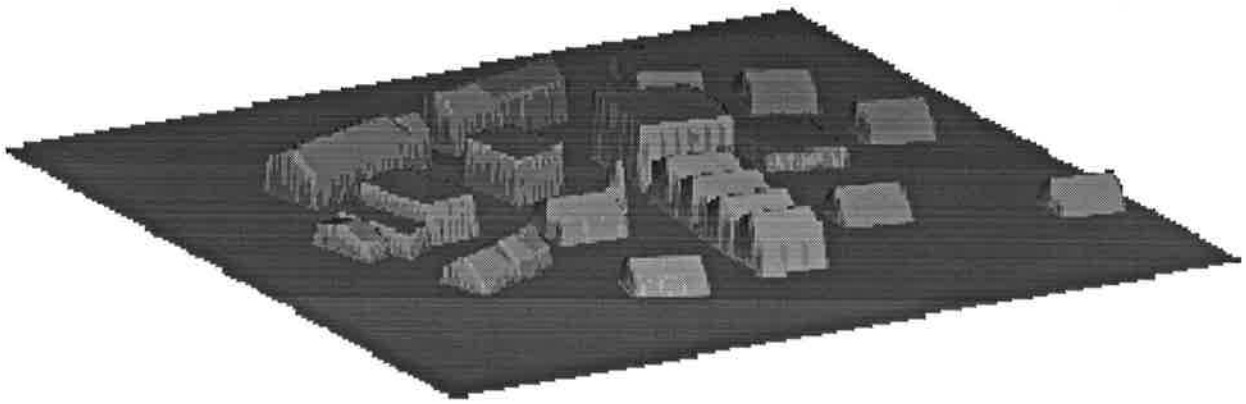

Figure 10. Shaded view of the ground truth model corresponding to the testsite. The area covers approximately 160 x 120 m^2.

From this new site model it was possible to calculate the areas and mean height of each building and compare the measurements to the ground truth data. The results can be seen from Table 1.

Table 1. Areas and mean height measurements of the extracted building models compared to ground truth (GT) data.

Bldg.	Area in m^2			Mean Height in m		
	GT	Model	Error	GT	Model	Error
A	316.6	326.0	+9.4	7.11	7.46	+0.35
B	228.0	236.2	+8.2	7.84	9.09	+1.25
C	144.5	172.4	+27.9	7.54	7.06	-0.48
D	93.8	117.9	+24.1	4.70	3.98	-0.72
E	347.4	349.2	+1.8	5.69	5.78	+0.09
F	146.7	115.9	-30.7	7.50	5.57	+0.07
G	286.5	226.1	-60.4	10.58	10.72	+0.14
H	206.5	196.2	-10.3	2.85	4.80	+1.95
I	98.4	99.3	+0.8	4.54	5.29	+0.75
J	171.1	185.1	+14.0	3.84	3.69	-0.15
K	129.1	117.8	-11.4	5.07	5.06	-0,01
L	442.4	452.5	+10.2	7.79	8.40	+0.61
M	97.7	107.0	+9.3	4.04	3.84	-0.20
N	93.7	106.0	+12.3	4.26	3.96	-0.30
O	95.6	100.4	+4.8	3.78	3.54	-0.24
RMS			± 21.46			± 0.70

6. DISCUSSION AND OUTLOOK

In this paper we have demonstrated that the detection and reconstruction of buildings from multiple view interferometric and slant range SAR data is feasible. Combination of multiple views, fusion of results gained from different data types and especially simulation of interferometric and slant range SAR data helped us to understand the various phenomena and to accomplish the goal.

Comparing the resulting site model from Fig. 9 to the ground truth data (Fig. 10) just a view differences occur. Apart from the steeple of the church K (cf. Fig. 4 for building letters) and the compound buildings E and L, where our simple building models are not sufficient to describe the shape, only two building models are obviously wrong, namely building B and F. In case of building B a flat roof is assigned instead of the correct gable roof and in case of building F a gable roof is assigned instead of the correct flat roof. Both mismatches result from occlusion phenomena caused by the adjacent building G, which is the topmost building on the site. So within the limits of the used three simple building models (flat roofed and gable roofed in two directions) the results are quite promising, especially because no manual interaction was needed during the extraction procedure. Comparing the area and mean height values of the extracted building models to the ground truth model (see Table 1) the resulting RMS errors are $\pm 21.46m^2$ for the area and $\pm 0.70m$ for the mean height which lie within the range of 3 times the resolution of $0.3m$.

Further refinements of the building models should be possible by feeding this new model once more back into the simulator and comparing the shape of the resulting shadow areas to the original slant range SAR magnitude images.

ACKNOWLEDGMENTS

The authors wish to thank SANDIA for providing the SAR images and Bob Wilson from Vexcel Corporation for providing the ground truth data.

REFERENCES

1. K. Hoepfner, A. Hanson, and E. Riseman, "Recovery of Building Structure from SAR and IFSAR Images," in *ARPA Image Undertanding Workshop*, pp. 559–563, Morgan-Kaufmann, 1998.
2. R. Xiao, C. Lesher, and B. Wilson, "Building Detection and Localization Using a Fusion of Interferometric Synthetic Aperture Radar and Multispectral image," in *ARPA Image Understanding Workshop*, pp. 583–588, Morgan-Kaufmann, 1998.
3. G. R. Burkhart, Z. Bergen, and R. Carande, "Elevation Correction and Building Extraction from Interferometric SAR Imagery," in *Proceedings of IGARSS'96*, pp. 659–661, IEEE, Lincoln, Nebraska, 1996.
4. P. Gamba, B. Houshmand, and M. Saccani, "Detection and Extraction of Buildings from Interferometric SAR Data," *IEEE Transactions on Geoscience and Remote Sensing* **38**, pp. 611–618, January 2000.
5. X. Y. Jiang and H. Bunke, "Fast segmentation of range images into planar regions by scan line grouping," *Machine Vision and Applications* **7**, pp. 115–122, 1994.
6. U. Soergel, U. Thoennessen, H. Gross, and U. Stilla, "Segmentation of Interferometric SAR Data for Building Detection," in *International Archives of Photogrammetry and Remote Sensing*, vol. XXXIII, Amsterdam, 2000.
7. U. Soergel, K. Schulz, and U. Thoennessen, "Enhancement of Interferometric SAR Data Using Segmented Intensity Information in Urban Areas," in *Proceedings of IGARSS'00*, IEEE, Honolulu, Hawaii, 2000. CD-ROM.
8. U. Sörgel, K. Schulz, and U. Stilla, "3D-Visualization of Interferometric SAR Data," in *Proceedings of 3rd European Conference on Synthetic Aperture Radar, EUSAR*, pp. 305–308, VDE Verlag, Berlin, Offenbach, München, Germany, 23-25 May 2000.
9. R. Bolter, "Reconstruction of Man-Made Objects from High Resolution SAR Images," in *Proceedings of IEEE Aerospace Conference*, (Big Sky, Montana, CD-ROM, Paper No.: 6.0305), 2000.
10. R. Bolter and F. Leberl, "Phenomenology-Based and Interferometry-Guided Building Reconstruction from Multiple SAR Images," in *Proceedings of EUSAR*, pp. 687–690, (München, Germany), 2000.
11. R. Bolter and F. Leberl, "Detection and Reconstruction of Human Scale Features from High Resolution Interferometric SAR data," in *Proceedings of ICPR 2000*, (Barcelona, Spain).
12. R. Bolter and F. Leberl, "Shape-from-Shadow Building Reconstruction from Multiple View SAR Images," in *Applications of 3D-Imaging and Graph-Based Modeling 2000, 24th Workshop of the Austrian Association for Pattern Recognition (ÖAGM/AAPR)*, R. Sablatnig, ed., pp. 199–206, Österreichische Computer Gesellschaft, Band 142, Villach, Austria, 2000, Best Presentation Award.